Improved Toughness of Polylactide by Binary Blends with Polycarbonate with Glycidyl and Maleic Anhydride-Based Compatibilizers

Ramon Tejada-Oliveros, Jaume Gomez-Caturla,* Lourdes Sanchez-Nacher, Nestor Montanes, and Luis Quiles-Carrillo

This work reports on the development of polylactide (PLA) and polycarbonate (PC) blends with different compatibilizers with enhanced toughness. Since both polymers are immiscible, two types of compatibilizers are tested: petrochemical-based copolymers Xibond 160 and Xibond 920 with maleic anhydride and epoxy groups, respectively, and natural-based compatibilizers with the same functionalities, namely maleinized linseed oil (MLO) and, epoxidized linseed oil (ELO). Mechanical, thermal, and morphological characterization shows better properties for the PLA/PC (80/20 wt%) blends with chemically modified natural oils (ELO and MLO). The addition of 5 phr (parts per hundred resin) of MLO gives the maximum values for impact strength and elongation at break. Moreover, the glass transition temperature (T_g) slightly decreases with the addition of natural compatibilizers, thus showing some plasticization effect. Petroleum-derived compatibilizers give interesting results regarding tensile strength and stiffness without plasticization. PLA/PC blends show higher thermal stability than neat PLA, regardless of the compatibilizer used, since PC is much more thermally stable than PLA. The obtained results indicate that both petroleum-based and natural-derived compatibilizers positively contribute to enhance the properties of the binary PLA/PC blends. Nevertheless, the results with MLO suggest this is an interesting biobased solution to provide increased toughness to PLA/PC blends.

1. Introduction

In the last years, the so-called biopolymers have been taken over more market share. These polymers possess similar physical, mechanical, chemical, and thermal properties to traditional polymers, thus becoming suitable solutions for a sustainable development. Furthermore, from an industrial point of view, the fact that they can be processed using the same equipment as for traditional polymers (extrusion, injection, sheet moulding, blow moulding, and so on), has increased their acceptance toward manufacturers. The main drawback of these biopolymers is still their price. Although technologies and manufacturing processes of these materials have been optimized over the last years, the price of biopolymers is much superior compared to that of traditional petroleum-based polymers.

Within all biopolymers, the biodegradable ones are attracting especial interest. They can be considered environmentally friendly materials with a positive effect on sustainable development.[1] At the end of their lifetime, they can undergo disintegration in controlled compost soil. The products from this disintegration process are water, CO_2, and/or methane altogether with biomass, which contribute to close the life cycle. In addition, this factor makes it possible to obtain highly environmentally efficient products, which end their life cycle without generating waste. However, from a technological and industrial point of view, this composting could generate certain controversy. It must be noted that the composting conditions require some energy expense, processing costs, investment on installations, and so on, in order to obtain a "product" that lacks market value. Despite being an environmentally friendly process, it does not present economic advantages compared to recycling or other upgrading strategies. These strategies are very much focused on single-use plastics, but both sides have to be taken into account. Moreover, it must be noted that it is an expensive material, as it has been previously stated. This is the reason for which mechanical recycling continues to be the optimal option to treat polymeric materials at the end of their lifetime, regardless of those being biopolymers.

R. Tejada-Oliveros, J. Gomez-Caturla, L. Sanchez-Nacher, N. Montanes,
L. Quiles-Carrillo
Instituto de Tecnología de Materiales (ITM)
Universitat Politècnica de València (UPV)
Plaza Ferrándiz y Carbonell 1, Alcoy 03801, Spain
E-mail: jaugoca@epsa.upv.es

**ADVANCED
SCIENCE NEWS**

www.advancedsciencenews.com

**Macro-
molecular
Materials and Engineering**

www.mame-journal.de

Through mechanical recycling, biopolymers can be reprocessed with new shapes and designs suitable to new applications.[2,3]

On the other hand, it should be considered that blending is a common practice in the field of polymers. The advantages regarding the properties of blends are widely known. In the case of biopolymers, it is also a usual mechanism to optimize their properties. Furthermore, due to the high cost of biopolymers, it is very common to blend them with other cost-effective traditional polymers to produce blends, with the objective of reducing the cost of the material at the same time its properties can be improved. In this case, mechanical recycling after consumption gains special value, while compost would not make any sense from an industrial point of view. It is worthy to remark that disintegration in controlled compost soil offers important benefits to the environment but, from an industrial point of view, the cost of biodegradable polymers is still high, and it is preferable to upgrade them before disintegration.

It is widely known that one of the most used biopolymers nowadays is polylactic acid (PLA). According to European Bioplastics, in 2020 the production of PLA reached 18.7% of the worldwide biopolymer production of 2.11 million tons. PLA is obtained through fermentative processes from sugar-rich biomass, cellulose, and starch. Some examples of these natural resources could be sugarcane, potato, wheat, and other renewable wastes or biomass.[4–6] PLA obtained from these sources has similar mechanical and thermal properties to those of a commodity polystyrene (PS). PLA is an aliphatic polyester with a semicrystalline structure and typical glass transition and melting temperatures of 60 °C and 175 °C, respectively. Its main weaknesses are its fragility and low toughness, as well as its high glass transition temperature, which reduces the processing temperature range.[7] One of the most important application fields for PLA nowadays is 3D printing.[8] It is also used in catering disposable elements, food packaging, biomedical applications (stents, sutures, medical devices, among others) or even sensors.[9–14]

Many investigations on PLA blends have focused on improving its toughness by combining it with other polymers. Nofar et al. developed a wide revision of the possibilities of obtaining PLA blends with a wide range of polymers: polyethylene (PE), polypropylene (PP), PS, acrylonitrile butadiene styrene (ABS), polyethylene terephtalate (PET), polybutylene terephtalate (PBT), polyoxymethylene (POM), among others.[4,15,16] In most of the cases, polymers, either biodegradable or synthetic, show partial miscibility or full immiscibility with PLA. For this reason, most investigations have focused on the use of compatibilizers with the objective of improving the properties of PLA-based blends.[17] These works have reported modifications in the T_g of PLA, improvements in toughness, flexibility and impact strength, among other properties. Other studies have focused on the incorporation of traditional polymers rather than biopolymers into PLA, since traditional petroleum-derived polymers are cheaper. In this field, Imre et al. developed PLA blends with PS and polymethyl methacrylate (PMMA), obtaining blends with suitable properties for electronic and automotive industries.[18] The addition of polypropylene carbonate (PPC) into PLA provides improved elongation at break, although both polymers are immiscible.[19] PLA blends with polyethylene (PE) also offer improved toughness.[3,20] The effect of polyamide 6,10 (PA610) on the crystallinity of PLA was studied by Keridou et al.[21] PLA blends with PP present bet-

ter mechanical behavior besides improving thermal stability in comparison with neat PLA.[22–24] The addition of PS into PLA improves the processability of the blends and their mechanical properties.[25,26]

PLA blends with polycarbonate (PC) have gained increasing interest. Usually, the addition of PC to PLA leads to an improvement of thermal stability, tensile strength, and elongation at break and, subsequently, PLA toughness. In particular, this blend can find applications in technologic fields such as electronics (mobile phones), automotive industry, computers, and so on. Being two immiscible polymers, some research works have focused on the use of compatibilizers to achieve the abovementioned properties.[4,16,27–34] Chelghoum et al. followed a different approach to improve the compatibility of PLA and PC in their blends. They promoted transesterification reactions between PLA and PC by adding samarium acetylacetonate (Sm-Acac) to catalyze interchange reactions between them. Their results showed a plasticizing effect that diminishes both glass transition temperatures of neat polymers in the blend, as well as a decrease in the melting peak temperature and the degree of crystallinity of PLA.[35]

Dicumyl peroxide (DCP), a free radical initiator and cobalt (II) acetylacetonate were used by Hedayati et al. to favor the interaction between PLA/PC blends and nanoclay.[28] Lee et al. analyzed the compatibilizing effect of different copolymers, namely poly(styrene-g-acrylonitrile)-maleic anhydride (SAN-g-MAH), poly(ethylene-co-octene) rubber-maleic anhydride (EOR-MAH), and poly(ethylene-co-glycidyl methacrylate) (EGMA), in PLA/PC blends with a clear improvement on toughness, particularly with SAN-g-MAH copolymer.[15] With a similar approach, Qu et al. added ethylene-maleic anhydride-glycidyl methacrylate terpolymer (EMG) as compatibilizer and talcum powder as nucleant to improve the overall performance of PLA/PC blends.[33,36] The work of Phuong et al. optimized the addition of tetrabutylammonium tetraphenylborate (TBATPB) and triacetin in a PLA/PC blend. The compatibilizing effect of these additives improved both mechanical and thermal properties. They reported improved interaction between PLA and PC that was responsible for the aforementioned improvement.[32] Wang et al. also used a copolymer, poly(butylene succinate-co-lactate) (PBSL) and epoxy (EP) as compatibilizers in PLA/PC blends, attaining an improvement in toughness and thermal resistance.[16] Geng et al. focused their work on the optimization of printability and processability PLA/PC blend for fused deposition modeling (FDM) applications by adding a warpage modifier terpolymer (ethylene-butyl acrylate-glycidyl methacrylate).[8]

The aim of this work is to improve the compatibilization of PLA and PC, developing PLA/PC blends with compatibilizing compounds that have not been tried before in this case, in order to improve the interaction between both polymers and, subsequently, their toughness. Furthermore, petrochemical and natural compatibilizers are tested and compared with each other in this study. Maleic anhydride and glycidyl functionalities, which are highly reactive with both polymers, are used in this work to improve the interactions in PLA/PC blends with a constant PC content of 20 wt%. The potential of two petroleum-derived copolymers, namely Xibond 160 and Xibond 920, which possess the aforementioned functionalities, is compared with chemically modified linseed oil, with the same functional groups:

**ADVANCED
SCIENCE NEWS**

www.advancedsciencenews.com

{M} acro-
molecular

Materials and Engineering

www.mame-journal.de

Table 1. Summary of the mechanical properties of the injection-molded samples of uncompatibilized and compatibilized polylactide (PLA)/polycarbonate (PC) blends. Tensile modulus (E), maximum tensile strength (σ_{max}), and elongation at break (ϵ_b), Shore D hardness, and impact strength (Charpy's test).

Code	E [MPa]	σ_{max} [MPa]	ϵ_b [%]	Shore D hardness	Impact strength [kJm^{-2}]
PLA	3107 ± 109	45.5 ± 1.2	9.0 ± 0.6	81.6 ± 0.5	3.0 ± 0.4
PLA/PC	2794 ± 101	33.2 ± 0.4	5.6 ± 0.3	80.4 ± 1.1	2.8 ± 0.2
PLA/PC/Xibond920	2826 ± 53	34.8 ± 2.6	6.9 ± 1.4	76.0 ± 0.7	3.0 ± 0.1
PLA/PC/Xibond160	3355 ± 153	41.5 ± 2.0	6.0 ± 0.5	81.8 ± 1.3	2.3 ± 0.1
PLA/PC/ELO	2974 ± 39	13.2 ± 1.1	8.6 ± 1.6	79.2 ± 0.8	4.3 ± 0.2
PLA/PC/MLO	2988 ± 25	42.1 ± 1.4	9.2 ± 0.1	79.0 ± 0.7	4.8 ± 1.0

maleinized linseed oil (MLO) and epoxidized linseed oil (ELO). The effects of this set of compatibilizers on mechanical properties (tensile, impact and, hardness) of PLA/PC blends are evaluated, as well as their effect on thermal behavior by differential scanning calorimetry (DSC), thermogravimetric analysis (TGA) and dynamic mechanical thermal analysis (DTMA). The effects of the reactive compatibilization of these maleinized and epoxidized compounds on the morphology of the PLA/PC blends are also studied by field emission scanning electron microscopy (FE-SEM).

2. Results

2.1. Mechanical Properties

Table 1 sums up the mechanical results of neat PLA, PLA/PC blend, and PLA/PC blends with different compatibilizers.

As it can be observed, the high values of tensile modulus and tensile strength, altogether with a low value of elongation at break, are typical for neat PLA, as it has been reported by other authors.[28,37] The uncompatibilized PLA/PC blend with 20 wt% PC shows a decrease in these three mechanical properties. The tensile modulus slightly decreases down to 2794 MPa, tensile strength is 27% lower, while elongation at break decreases considerably down to 5.6%, which means a decrease of 38% in relation to neat PLA. These results indicate that PLA/PC blend is a rigid and brittle material. Considering that neat PC offers high values of elongation at break (154%), its addition to PLA was initially expected to improve its toughness. However, the mechanical properties of the PLA/PC blend were lower than those of neat PLA, which suggests immiscibility between these two polymers as reported in literature.[33,34,38,39]

The use of compatibilizers into the PLA/PC blend can enhance its mechanical performance. The tensile modulus and tensile strength increased with addition of both Xibond 920 and Xibond 160 into the PLA/PC blend, especially in the case of the maleic anhydride-based copolymer, Xibond 160, which increased tensile modulus and tensile strength up to values of 3355 and 41.5 MPa, respectively. This suggests that maleic anhydride could improve the interaction between PLA and PC compared to the glycidyl-functionalized copolymer (Xibond 920). It is worthy to highlight the tensile strength that the Xibond 160 compatibilized sample presents, which is slightly lower than that of neat PLA and much higher than the uncompatibilized PLA/PC blend, thus implying that this copolymer compatibilizes the base PLA/PC blend. Fur-

thermore, the addition of these copolymers also provides a slight increase in the elongation at break, which is also representative for some compatibilization effect reaching values of 6.9% and 6.0% for blends with Xibond 920 and Xibond 160, respectively, in comparison with the 5.6% value for PLA/PC. This improvement in ductile behavior and mechanical tensile resistance was an indicative of the compatibilizing effect that maleic anhydride- and glycidyl-based copolymers can provide to PLA/PC blend. Both functional groups in Xibond 160 and Xibond 920 can react with hydroxyl end groups present in the aliphatic polyester chains, as well with terminal groups in condensation PC polymer chains.[40] Therefore, the use of these two copolymers can enhance the properties of PLA-based blends.

Table 1 also shows the effects of the two biobased compatibilizers from linseed oil. As it can be seen, it is again the maleic anhydride functionalized linseed oil (MLO), which gives the best-balanced properties, since the tensile modulus and tensile strength are increased up to 2988 and 42.1 MPa, respectively, which are quite higher than that of PLA/PC. In a parallel way, the elongation at break is improved up to 9.2% which is noticeably higher than the base PLA/PC blend and, even higher than the elongation at break of neat PLA, which is 9%. The effect of the glycidyl functionalized linseed oil is not so remarkable in terms of the tensile strength since it decreases down to 13.2 MPa which suggests that, together with compatibilization, ELO provides a clear plasticization effect on PLA as previously reported.[41,42] On the other hand, the tensile modulus increases in relation to the PLA/PC blend, from 2794 to 2974 MPa, as well as elongation at break, which improves from 5.6% for PLA/PC, to 8.6% for PLA/PC/ELO, demonstrating certain plasticization. Some works reported the multifunctionality of MLO, which is responsible for the increase in ductility of PLA due to a combination of plasticization, chain extension, branching, and cross-linking phenomena.[33,43–45] In spite of the fact that ELO and MLO can improve the ductile properties, the petroleum-based compatibilizers give higher tensile strength values which is representative for better cohesion while both ELO and MLO, in addition to the compatibilization effect, also provide plasticization. The presence of ELO and MLO enhances the mobility of the polymeric chains of PLA with a slight plasticization effect.[41,42]

Table 1 also gathers the impact strength results for each one of the samples. Similarly to the results of the tensile test, the blend of PLA with 20%wt of PC presents low impact strength, 2.8 kJm^{-2}, due to its brittle behavior. It must be kept in mind that neat PLA is a very brittle polymer with low impact strength (3.0

**ADVANCED
SCIENCE NEWS**

www.advancedsciencenews.com

**Macro-
olecular
Materials and Engineering**
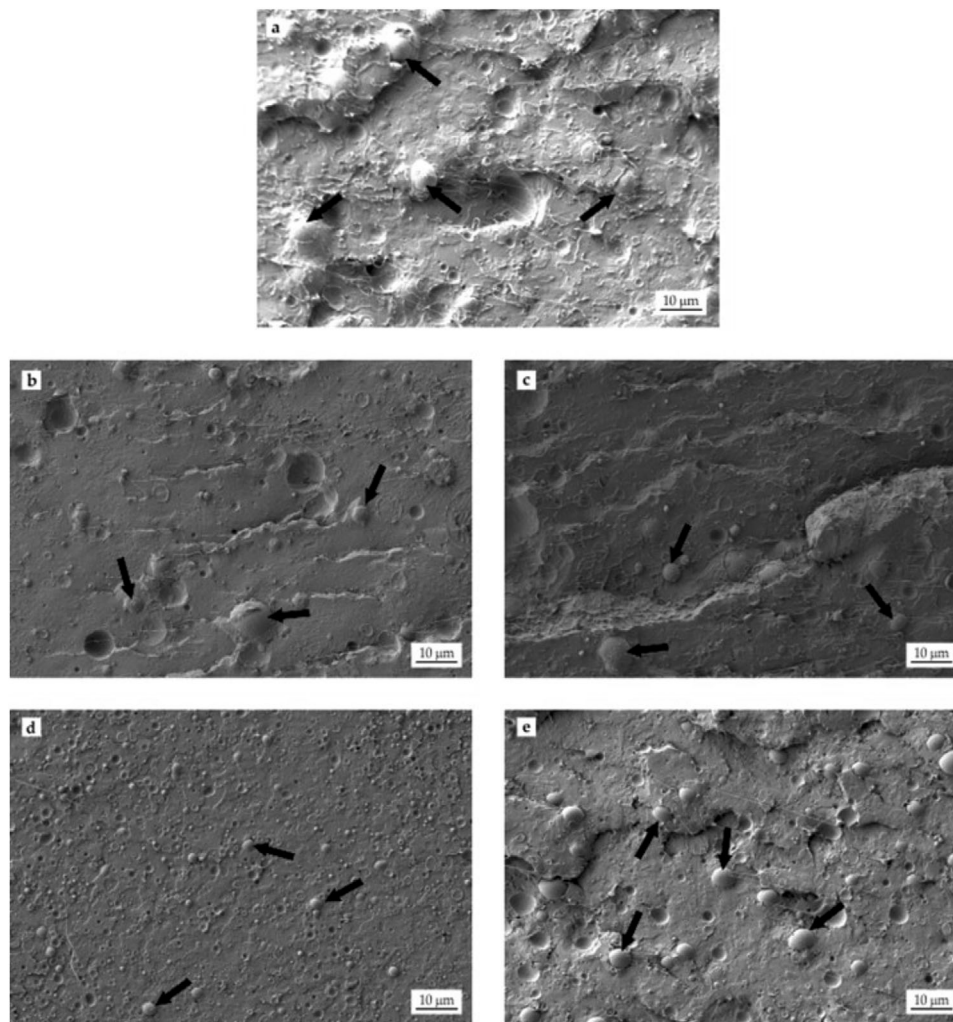
www.mame-journal.de

Figure 1. Field emission scanning electron microscopy (FESEM) images of the impact fracture surfaces at 1000x: a) polylactide (PLA)/polycarbonate (PC), b) PLA/PC/XIBOND920, c) PLA/PC/XIBOND160, d) PLA/PC/ELO, and e) PLA/PC/MLO.

kJm^{-2}); nevertheless, neat PC is a high toughness engineering polymer with a high impact strength. As observed, the uncompatibilized blend shows even lower impact strength values than neat PLA which remarks the lack of miscibility between these two polymers.[16,29,30,33] Despite both Xibond compatibilizers give an important increase in the tensile strength, toughness is not improved so much, with a value of 3.0 kJ m^{-2} for Xibond 920 and a very low value of 2.3 kJm^{-2} for Xibond 160. However, both linseed oil derivatives provide a clear increase in the impact strength up to values of 4.3 and 4.8 kJm^{-2} for ELO- and MLO-compatibilized PLA/PC blends, respectively. These values are much higher than neat PLA, thus showing the potential of these two linseed oil derivatives as compatibilizers in PLA/PC blends with improved toughness.

On the other hand, Shore D values did not vary significantly. The PLA/PC blend presented a value of 80.4 HS$_D$, which is slightly lower to that of neat PLA (81.6 HS$_D$). With the addition of styrene-based copolymers with maleic anhydride and glycidyl groups, a slight increase in the Shore D hardness can be observed but it is not so significant, which is in accordance with the pre-

viously mentioned tensile properties. Regarding the use of modified linseed oil, hardness results are slightly lower with values of about 79 HS$_D$. This could be related to the plasticization effect that these chemically modified linseed oil has on PLA.

2.2. Morphology of PLA/PC Blends

Figure 1 shows the morphology of the fractured surface of impact test samples of PLA/PC blends with different compatibilizers. The morphology of the uncompatibilized PLA/PC blend proves to be heterogeneous. Two phases can be differentiated: the continuous PLA matrix phase and the dispersed phase with spherical shapes, which corresponds to the PC-rich phase (marked with black arrow). This phase separation is representative for the immiscibility of PLA and PC.[16,18,27,34,35] The size of the dispersed spheres is considerable (with diameters above 5 µm) and they are uniformly dispersed in the PLA matrix phase. As reported by Yemisci et al., the lack of interaction between both polymers leads to formation of the typical droplet-like binary structure with

**ADVANCED
SCIENCE NEWS**

www.advancedsciencenews.com

⎡M⎤ acro-
molecular
Materials and Engineering

www.mame-journal.de

PC spherical particles embedded into the PLA matrix.[18,34] On the other hand, spherical voids are also observed during impact fracture due to the phase separation between PLA and PC. The spherical particles are pulled out from the matrix during fracture, leaving a spherical void. This lack of miscibility between both polymers is responsible for the previously commented poor mechanical properties. The lack of interaction between the PLA matrix and the embedded PC-rich phase does not allow appropriate stress transfer. Consequently, the blend offers poor cohesion and, subsequently, it is more brittle compared with neat PLA.

The addition of Xibond copolymers with different functionalities has some interesting effects on the morphology of the compatibilized PLA/PC blend. Despite the phase separation is still detectable, it seems the morphology is less rough and somewhat increased continuity is detected with PC-rich phase being more embedded into the PLA matrix. This has a positive effect on stress transfer and, subsequently, mechanical properties related to cohesion are improved, as previously described with regard to tensile strength. Nevertheless, the PC-rich phase is not remarkably reduced, and the droplet size ranges from 3 to 6 µm. Nevertheless, the PLA/PC blends compatibilized with the maleic anhydride-based copolymer seems to offer more continuity and cohesion between the PC droplets and the surrounding PLA matrix.

Regarding the addition of linseed oil derivatives (ELO and MLO), the blends still exhibit phase separation, but two different morphologies can be clearly observed. The MLO-compatibilized PLA/PC blend shows the same drop-like phase separation with an average PC-rich domain size of 5 µm, but compatibilization with MLO leads to a reduction of the gap between the PC-rich phase and the surrounding PLA-rich matrix. The ELO-compatibilized PLA/PC blend shows a noticeable change in morphology since the droplet size of the PC dispersed phase is remarkably reduced to an average diameter of 3 µm. This suggests better interaction between PLA and PC.[15,18,24,34] This structure is responsible for the improved impact strength since the interaction between PLA and PC is improved.[29,33] In addition to the compatibilization effect, both ELO and MLO provide some plasticization effect due to their structure. This plasticization phenomena occurs thanks to the fact that the plasticizer molecules (ELO and MLO) locate between different base polymer chains, acting as lubricants and increasing the free volume between the chains, providing them with more mobility. Thus increasing ductility in the polymer. Additionally, ELO and MLO can react with hydroxyl groups placed at the end groups of PLA polymer chains, inducing a chain extension effect.[33,43–45]

2.3. Thermal Properties of PLA/PC Blends

Figure 2 shows the DSC thermograms of neat PLA, neat PC, uncompatibilized, and compatibilized PLA/PC blends. The only thermal transition present in the DSC thermogram of neat PLA is a slight step in the base line at 62.5 °C, which is ascribed to the glass transition phenomenon in the polymer, corresponding this step to its glass transition temperature (T_g). This PLA grade is amorphous and, subsequently, no cold crystallization and melting peaks are observed. With regard to neat PC, since it is also an amorphous polymer, it only presents its glass tran-
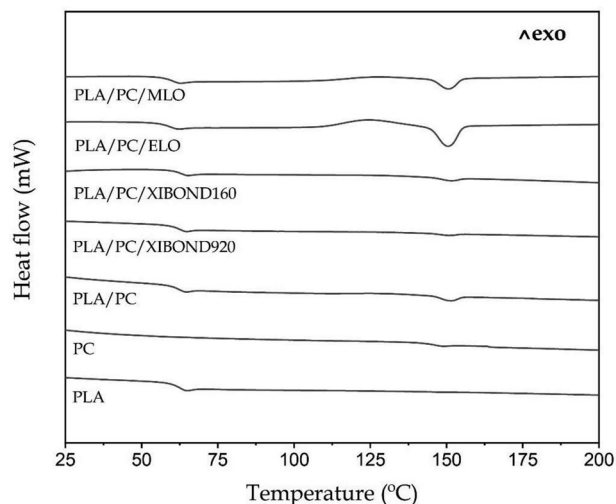

Figure 2. Differential scanning calorimetry (DSC) thermograms of polylactide (PLA)/polycarbonate (PC) blends with different compatibilizers.

sition temperature (T_g), located at about 150 °C. With regard to the T_g values of the PLA-rich phase in PLA/PC blends, very slight changes can be observed by using different compatibilizers. The T_g for the uncompatibilized PLA/PC blend is located at 62.2 °C which is representative for immiscibility.[27,28,34,35] Compatibilization with styrene-functionalized polymers do not produce a remarkable change in the T_g of the PLA-rich phase which remains at values of 62.2 °C and 62.5 °C for PLA/PC blends with Xibond 920 and Xibond 160, respectively. With regard to the linseed oil derivatives, the T_g of the PLA-rich phase is slightly reduced to 59.3 °C and 60.1 °C for the ELO- and MLO-compatibilized PLA/PC blends, which is in accordance with the slight plasticization both modified vegetable oils provide as described by Ferri et al.[45] An interesting phenomenon can be observed in uncompatibilized PLA/PC blend. A slight endothermic peak can be seen at about 150 °C which is attributed to induced PLA crystallization by presence of PC.[27,34]

This phenomenon is much more pronounced by suing both MLO and ELO compatibilizers. This phenomenon is even more accentuated in PLA/PC blend with ELO. In fact, a wide cold crystallization peak can be detected with a peak temperature of 125 °C and, a clear melting peak is observed with a maximum melt rate peak located at 150 °C, which overlaps with the T_g of the PC-rich phase. Therefore, by conventional DSC it is not possible to separate both thermal transitions and quantitatively characterize the main parameters such as melting enthalpy,[16,35] but it can be detected an induced crystallization of PLA by both linseed oil-based compatibilizers, probably due to an increase in the chain mobility. There is a synergetic effect in the increase in crystallinity between PC and the modified natural oils into neat PLA.

The TGA of the different materials allows to evaluate their thermal stability in a comparative way (**Figure 3**a), while Figure 3b shows the first derivative of the thermogravimetric curves (DTG). Additionally, **Table 2** gathers the main degradation parameters extracted from this test. The TGA curve corresponding to neat PLA shows a thermal degradation process in a single step. This degradation at high temperature is due to complex random scission
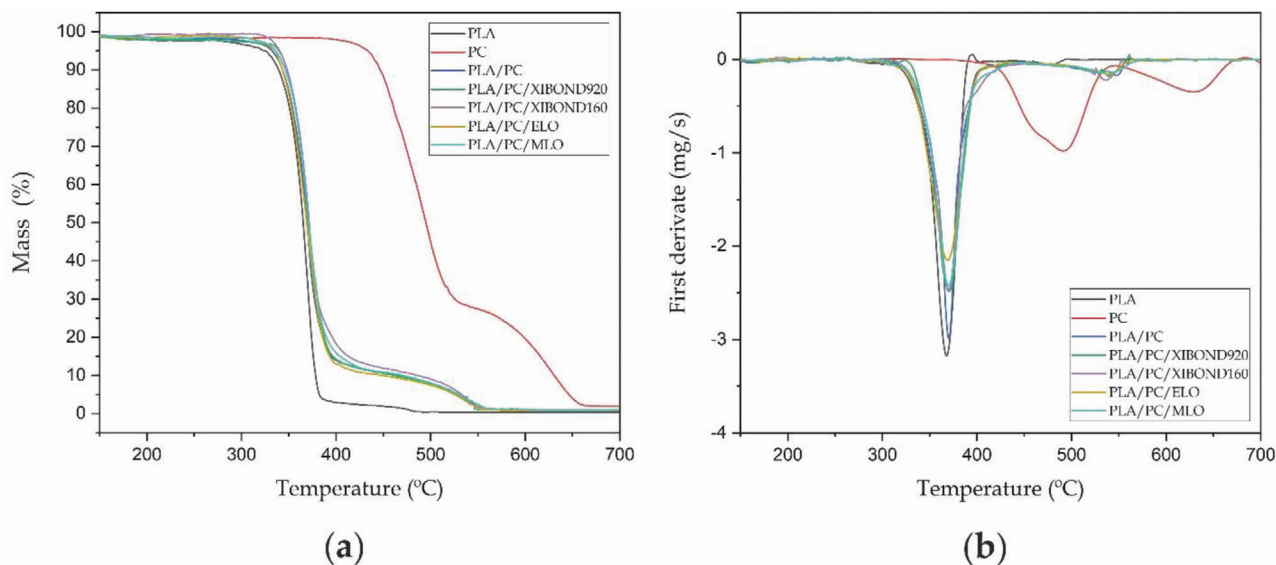
ADVANCED
SCIENCE NEWS
www.advancedsciencenews.com

[M] acro-
olecular
Materials and Engineering
www.mame-journal.de

Figure 3. a) Thermogravimetric analysis (TGA) curves and b) first derivative (DTG) of polylactide (PLA)/polycarbonate (PC) blends with different compatibilizers.

Table 2. Main thermal degradation parameters of the polylactide (PLA)/polycarbonate (PC) blends with different compatibilizers in terms of the onset degradation temperature at a mass loss of 5 wt% ($T_{5\%}$), maximum degradation rate (peak) temperature (T_{max}), and residual mass at 700 °C.

Code	$T_{5\%}$ [°C]	T_{max} [°C]	Residual weight [%]
PLA	323.3 ± 1.6	368.3 ± 2.1	0.3 ± 0.1
PC	434.3 ± 1.3	491.3 ± 1.8	1.9 ± 0.2
PLA/PC	332.3 ± 1.2	370.1 ± 1.6	0.9 ± 0.3
PLA/PC/XIBOND920	339.3 ± 1.4	371.3 ± 1.2	0.8 ± 0.2
PLA/PC/XIBOND160	340.9 ± 1.1	370.8 ± 0.9	0.9 ± 0.1
PLA/PC/ELO	335.3 ± 1.6	369.2 ± 1.4	0.8 ± 0.3
PLA/PC/MLO	335.8 ± 1.5	369.8 ± 1.2	0.8 ± 0.4

processes of the polymeric chains, altogether with depolymerization and transesterification as proposed by Hedayati et al.[28] Taking the onset degradation temperature as the one corresponding to a mass loss of 5%, neat PLA shows a degradation onset temperature of 323.3 °C, while the maximum degradation rate temperature is located at 368.3 °C which is in accordance to the results reported by Phuong et al.[32] On the other hand, neat PC presents a thermal degradation process in two steps, since the test has been carried out in air atmosphere, as it can be observed in the TGA curve.[32] Furthermore, its DTG plot presents two peaks corresponding to the maximum degradation rates of these two stages: 491 °C and 630 °C. As expected, PC showed very high thermal stability with an onset degradation temperature of 434.3 °C which is remarkably superior to that of neat PLA. Some authors have reported that PC presents a complex thermal degradation process, related to chemical reactions that take place between different functional groups present in its polymeric structure due to the ef-

fect of temperature. During the first stage in the thermo-oxidative degradation, complex chemical reactions take place: free radical scission from the PC polymeric chain from the isopropilidyene bond, branching reactions and cross-linking of molecular segments between oxygen bonds. Jang et al. reported that the first weight mass step in the TGA curve of PC is due to the oxidative scission of the carbon–carbon bond, hydrolysis reaction, and alcoholysis of the carbonate group. This first stage would happen between 450 °C and 560 °C in air atmosphere as suggested by Jang et al.[46] The oxygen in air atmosphere can promote branching reactions through free radicals after peroxide formation, and a highly reticulated structure with diaryl ester and insaturated C–C bonds above 440 °C.[32] The work of Song et al. reports that during PC degradation in an oxidant atmosphere, free radicals react, forming peroxides that can cross-link unsaturated diaryl and ether groups. The polyaromatic carbonous waste undergoes cross-linking reactions at high temperatures and degrades in a second stage, ranging from 550 to 800 °C.[32,46,47]

All PLA/PC blends show both steps: the first one corresponding to PLA and the second one to PC. The second degradation step is less pronounced since the main component of the developed blends is PLA.[35] It must be highlighted the improved thermal stability of the blends compared with neat PLA due to the presence of PC (**Table 3**).[28,32] The onset degradation temperature of the uncompatibilized PLA/PC blend is 332.3 °C, this is 10 °C higher than neat PLA. Both Xibond compatibilizers lead to a noticeable improvement on thermal stability since the onset degradation temperature is moved to values close to 340 °C for both styrene-based copolymer compatibilizers. In relation to the ELO- and MLO-compatibilized PLA/PC blends, a slight increase in the onset degradation temperature can also be observed with values around 335 °C. Regarding the maximum degradation rate temperature, all the PLA/PC blends show slightly superior values to that of neat PLA.

Table 3. Dynamic-mechanical properties of injection-molded samples of polylactide (PLA)/polycarbonate (PC) blends with different compatibilizers, at different temperatures.

Parts	E' [MPa] at 45 °C	E' [MPa] at 80 °C	$T_{g\ PLA}$ [°C][a]
PLA	820 ± 24	1.1 ± 0.1	63.1 ± 0.6
PLA/PC	749 ± 21	3.6 ± 0.2	63.9 ± 0.8
PLA/PC/XIBOND920	960 ± 17	15.5 ± 1.3	62.2 ± 0.7
PLA/PC/XIBOND160	1089 ± 26	3.4 ± 0.3	64.1 ± 1.1
PLA/PC/ELO	1050 ± 19	5.7 ± 0.6	60.6 ± 0.8
PLA/PC/MLO	1039 ± 25	1.7 ± 0.2	62.1 ± 0.5

[a] The T_g has been measured using the tan δ peak maximum criterion.

2.4. Dynamic-Mechanical Behavior of PLA/PC Blends

The evolution of the storage modulus, E', and the dynamic damping factor (tan δ), with the temperature were obtained by DMTA characterization (**Figure 4**). As it can be observed, the E' values at 40 °C are high for all the analyzed blends, as well as for neat PLA. In the 50 °C–70 °C range, an important decrease in E' was observed, which is ascribed to the PLA glass transition temperature (T_g). This change in the behavior of the material is due to the fact that below their T_g, blends and neat PLA present an elastic-vitreous behavior. Below the characteristic T_g of PLA, the uncompatiblized PLA/PC blend offers an E' value lower than neat PLA, while all other compatibilized PLA/PC blends are stiffer, with higher E' values. These values can be seen in Table 3 which gathers E' values at different temperatures for all the studied blends. At 45 °C, E' reaches a value of 749 MPa in the uncompatibilized PLA/PC blend while E' is higher in PLA/PC blends with both Xibond-based compatibilizers, with values of 960 and 1089 MPa for XIBOND 920 and XIBOND 160, respectively. In the case of the blends with natural compatibilizers, ELO and MLO, E' reaches values of 1050 and 1039 MPa, respectively. These results indicate an improvement in the stiffness of the base PLA/PC blend by using different compatibilizers, as previ-

ously observed by mechanical characterization. In the temperature range comprised between 50–70 °C, the α-relaxation of PLA occurs, which is associated with the activation of long-range coordinated molecular motions as reported by Cristea et al.,[48] reaching a first rubbery plateau region before cold crystallization. Nevertheless, since the used PLA grade is amorphous, very low cold crystallization is observed in the temperature range comprised between 90 °C and 110 °C. In the rubbery plateau region, at 80 °C the storage modulus has decreased dramatically to values of less than 10 MPa. Furthermore, in Figure 4b, the evolution of dynamic damping factor (tan δ) as a function of temperature can be observed for neat PLA and all PLA/PC blends developed in this study. The maximum values of tan δ are obtained for neat PLA. It is important to bear in mind that the dynamic damping factor, represents the ratio between the lost energy (E'') and the stored energy (E'), thus indicating PLA dissipates more energy than all other PLA/PC blends, since the maximum tan δ values for all PLA/PC blends are lower. Phuong et al. reported that the height of the tan δ peak is related to polymeric chains mobility.[49] It is worthy to note that the heights of tan δ peaks for uncompatibilized and compatibilized PLA/PC blends are lower than neat PLA thus showing more chain motion restriction, but the PLA/PC blend compatibilized with MLO shows the highest height of tan δ, compared to all other PLA/PC blends, which could be ascribed to the plasticization effect, as previously indicated. Despite there are several criteria to define the glass transition temperature, the maximum peak of tan δ, is widely approved. Table 3 also gathers the T_g values of the PLA-rich phase in all PLA/PC blends as well as for neat PLA. The T_g of the uncompatibilized PLA/PC blend (63.9 °C) hardly changes with regard to neat PLA (63.1 °C), thus showing their immiscibility. The use of styrene-based copolymer compatibilizers does not provide a decrease in the T_g values of the PLA-rich phase, with values of 62.2 °C and 64.1 °C for Xibond 920 and Xibond 160. The lower peak height of tan δ, also indicates a stiffer behavio as observed in tensile characterization. On the other hand, the ELO- and MLO-compatibilized PLA/PC blends show a slight decrease in the T_g of the PLA-rich phase, mainly detectable for the ELO-compatibilized blend with a T_g of
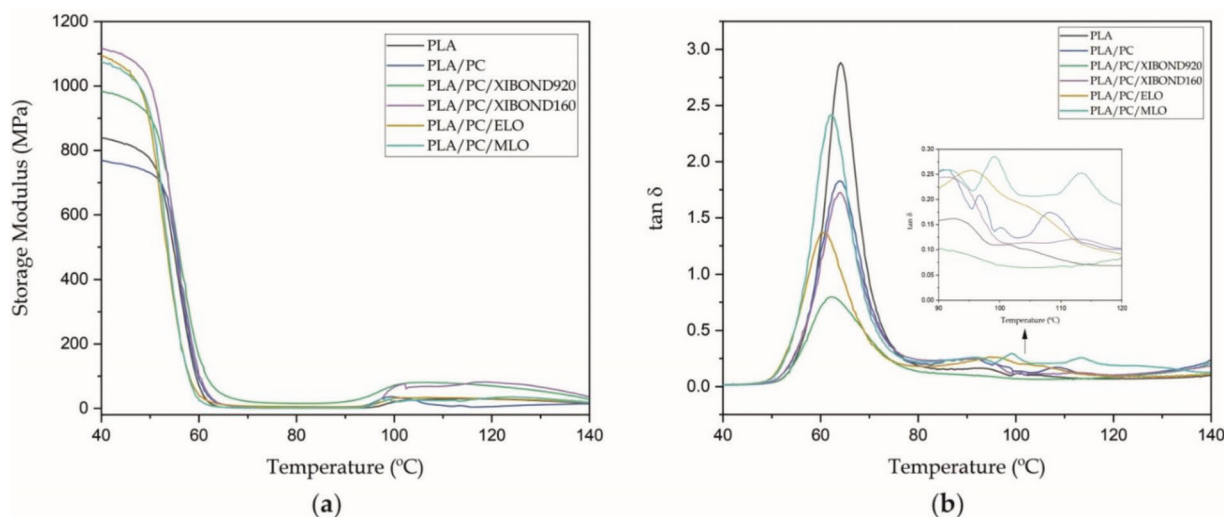

Figure 4. Plot evolution of a) the storage modulus (E') and b) the dynamic damping factor (tan δ) of the injection-molded samples of polylactide (PLA)/polycarbonate (PC) blends with different compatibilizers.
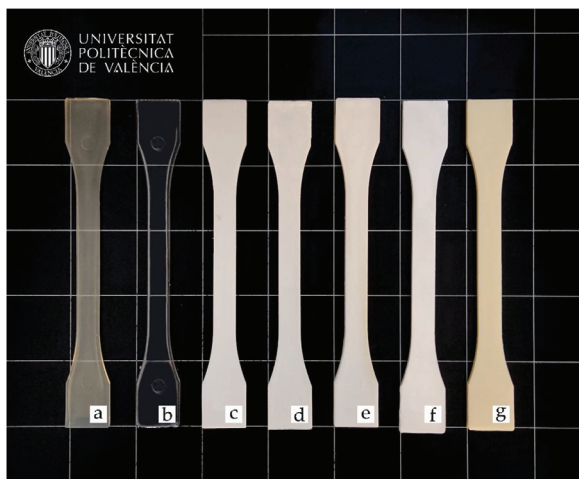
Figure 5. Visual appearance of the samples: a) neat polylactide (PLA); b) neat polycarbonate (PC); c) uncompatibilized PLA/PC; d) PLA/PC compatibilized with Xibond920; e) PLA/PC compatibilized with Xibond920; f) PLA/PC compatibilized with epoxidized linseed oil (ELO); and g) PLA/PC compatibilized with maleinized linseed oil (MLO).

Table 4. Luminance and color coordinates (L*a*b*) of the polylactide (PLA)/polycarbonate (PC) blends with different compatibilizers.

Code	L*	a*	b*	Yellowness index (YI)
PLA	40.8 ± 0.24	−0.44 ± 0.01	4.67 ± 0.12	21.3± 0.3
PC	55.9 ± 0.02	−0.60 ± 0.05	0.34 ± 0.02	6.2± 0.1
PLA/PC	89.2 ± 0.01	−0.09 ± 0.01	6.03 ± 0.01	17.0± 0.3
PLA/PC/Xibond920	87.9 ± 0.01	−0.23 ± 0.03	6.27 ± 0.02	17.5± 0.2
PLA/PC/Xibond160	88.4 ± 0.00	0.08 ± 0.01	6.75 ± 0.02	18.4± 0.3
PLA/PC/ELO	91.8 ± 0.02	−0.55 ± 0.02	4.34 ± 0.04	13.4± 0.1
PLA/PC/MLO	84.3 ± 0.00	0.49 ± 0.02	21.0± 0.02	43.5± 0.4

the PLA-rich phase of 60.6 °C, which is in accordance with the previous results obtained by DSC characterization.

2.5. Color Measurement and Wetting Properties of PLA/PC Blends

It must be noted that, for lots of technologic applications, the aesthetic and superficial appearance of the materials is a key factor to keep in mind when selecting the suitable material for a specific application. In this sense, **Figure 5** shows the visual appearance of the different studied materials. The clear transparency of the PC sample stands out. Despite the PLA grade is highly amorphous, it shows some transparency, but it is lower than that of neat PC. On the other hand, all PLA/PC blends are characterized by a lack of transparency, which is typical of polymer blends due to different refractive indexes of both polymers in the blend. All PLA/PC blends are opaque and have a white-color appearance. Some investigations relate this change in transparency of the polymer to a change in its internal structure. The polymeric

structures with biphasic formations due to immiscibility and/or certain degree of crystallinity, are responsible for this change to an opaque appearance due to differences in the refractive indexes of the immiscible phases.[50] This whitening can be quantified with the luminance value L* or clarity by measuring the color coordinates as shown in **Table 4.** (L* = 0 corresponds to black and L* = 100 stands for white). Whitening in the color of the material implies low values of the color coordinates a* b* and high values for the L* coordinate (the coordinates for pure white color L*, a *, b * are 100, 0 y 0, respectively). The values of L* coordinate are far superior for all the PLA/PC blends in comparison to neat PLA and PC samples. One important phenomenon to take into account is the yellowing that MLO provides, compared with all other compatibilizers. The quantification of this visual appearance is carried out through the yellowness index (YI). In particular, YI of the PLA/PC blend with MLO is the one with the highest value (43.5), which is far superior to the 13–18 values for the uncompatibilized PLA/PC and all other compatibilized PLA/PC blends.

Surface wettability can be another technological property to be considered in some applications. Generally, the intrinsically low surface energy that polymeric materials possess is related to their high hydrophobicity despite the presence of some polar groups. This hydrophobicity and, subsequently, the low surface energy plays a critical role in some processes such as creating adhesive joints, use of coatings, primers, sticking labels, ink printing, among others. A qualitative assessment of the wetting properties can be carried out by measuring the water contact angle (**Figure 6**). As it was expected, the surface of neat PLA, neat
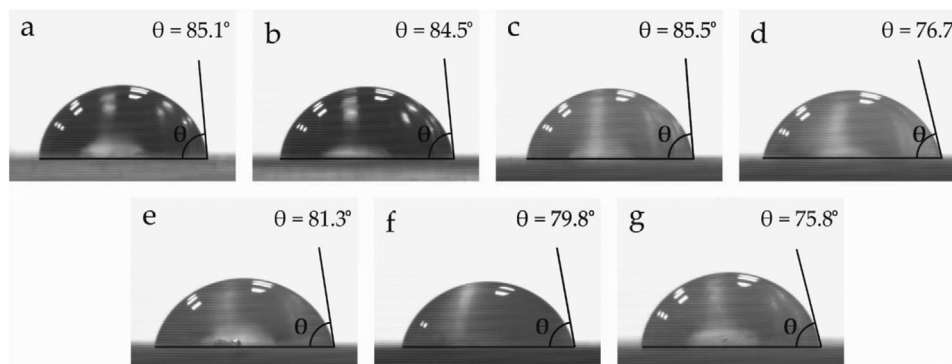

Figure 6. Water contact angle of the samples: a) polylactide (PLA); b) polycarbonate (PC); c) PLA/PC; d) PLA/PC/Xibond920; e) PLA/PC/Xibond160; f) PLA/PC/ELO; and (g) PLA/PC/MLO.

**ADVANCED
SCIENCE NEWS**

www.advancedsciencenews.com

{M}acro-
olecular

Materials and Engineering

www.mame-journal.de

PC, and the PLA/PC blend presents high water contact angles, with values around 85°. These means they are hydrophobic surfaces with low wettability. The addition of different compatibilizers with polar groups such as maleic anhydride and glycidyl functionalities leads to a slight increase in the wetting properties which is assessed by a slight decrease in the water contact angle. Despite all four compatibilizers provide a slight improvement in the wetting properties, it is worthy to note that the resulting surfaces are still hydrophobic. Therefore, additional surface treatments would be required to improve the adhesion.[51]

3. Conclusion

This works reports on the potential of blending PLA with PC as a technical approach to improve the low intrinsic toughness of neat PLA. Since PLA and PC are highly immiscible, the use of compatibilizers is required to achieve this improvement in toughness. This immiscibility is responsible for a decrease in all mechanical properties of PLA/PC without any compatibilizer. The use of styrene-based copolymers, namely Xibond 920 and Xibond 160 with glycidyl and maleic anhydride functional groups, provides an important increase in tensile strength due to improved polymer–polymer interaction. On the other hand, the use of chemically modified linseed oil with the same functional groups leads to interesting alternatives to petroleum-derived copolymers. ELO and MLO, respectively, provide a clear increase in the impact strength, thus contributing to reduce the intrinsic brittleness of neat PLA and its blend with PC. Both petroleum-based copolymers (Xibond) also provide improved thermal stability while ELO and MLO provide some plasticization phenomenon with a subsequent slight decrease in the glass transition temperature of the PLA-rich phase. Another important finding is that PC also promotes PLA crystallization with a synergistic effect of both modified linseed oils. As a general conclusion, it is worthy to note that blending PLA with PC is an interesting technical solution to improve the low intrinsic toughness of PLA which is one of the main drawbacks of using this polymer. Nevertheless, the immiscibility of both polymers requires the use of compatibilizers to enhance polymer–polymer interactions. Maleic anhydride- and glycidyl-functionalized materials represent an interesting solution to overcome this problem since both chemical groups are highly reactive toward PLA and PC with the subsequent improvement on polymer–polymer interaction.

4. Experimental Section

Materials: Polylactic acid (PLA) Ingeo Biopolymer 2003D grade was supplied by NatureWorks LLC (Nebraska, USA). This is a PLA grade for extrusion, with a density of 1.24 g cm^{-3} and a melt mass-flow rate of 6 g 10^{-1} min (measured at a temperature of 210 °C with a load of 2.16 kg). PC, Calibre 303-22 SC830104 grade was supplied by Trinseo (Michigan, USA). This grade possesses a density of 1.20 g cm^{-3} and a melt mass-flow rate of 22 g 10^{-1} min (measured at a temperature of 300 °C with a load of 1.2 kg).

Two petroleum-derived copolymers with maleic anhydride and glycidyl groups were kindly supplied by Polyscope Polymers BV (Geleen, Netherlands) with the tradename family Xibond. The maleic anhydride-based copolymer was Xibond 160, which is a styrene—maleic anhydride random copolymer with a molecular weight of 115 000 g mol^{-1} and an acid value of 250 mg KOH g^{-1}. With regard to the glycidyl-functionalized copolymer,

Xibond 920 was used. This is a styrene—glycidyl methacrylate random copolymer with a molecular weight of 50 000 g mol^{-1}.

Two chemically-modified linseed oil derivatives were used as biobased compatibilizers with the same functionalities contained in the petroleum-derived copolymers. These vegetable oil derivatives consisted on MLO that was supplied by Vandeputte (Mouscron, Belgium). This modified vegetable oil is characterized by a viscosity of 10 dPa s at 20 °C and an acid value comprised in the 105–130 mg KOH g^{-1} range. Regarding the glycidyl-functionalized vegetable oil, an ELO supplied by Traquisa S.L. (Barcelona, Spain) was used. This ELO has a density of 1.05–1.06 g cm^{-3} at 20 °C. Its epoxide equivalent weight (EEW) is 178 g equiv^{-1} and an acid value below 1 mg KOH g^{-1}. **Scheme 1** shows the chemical structure of all four compatibilizers used in this study.

Preparation of PLA/PC Blends: **Table 5** shows the composition of all developed blends. Prior to processing, all components were dried at 40 °C for 48 h in a dehumidifying dryer MDEO to remove residual moisture which could compromise processing and final properties. The corresponding components were weighed and premixed in a zipper bag. Then, the materials were fed into the main hopper of a co-rotating twin-screw extruder from Construcciones Mecánicas Dupra, S.L. (Alicante, España). This extruder has a screw diameter of 25 mm and a length-to-diameter ratio (L/D) of 24. The extrusion process was carried out at 20 rpm, setting the temperature profile, from the hopper to the die, as follows: 240-250-260-270 °C. The blends were then pelletized using an air-knife unit. In all cases, residence time was approximately 1 min. The pellets were then shaped into standard samples by injection molding in a Meteor 270/75 from Mateu & Solé (Barcelona, Spain). The temperature profile in the injection molding unit was (from the hopper to the injection nozzle): 240-250-260-270 °C. The cavity filling and cooling times were set to 1–10 s with a clamping force of 75 tons. Standard samples for mechanical and thermal characterization with a nominal thickness of 4 mm were obtained.
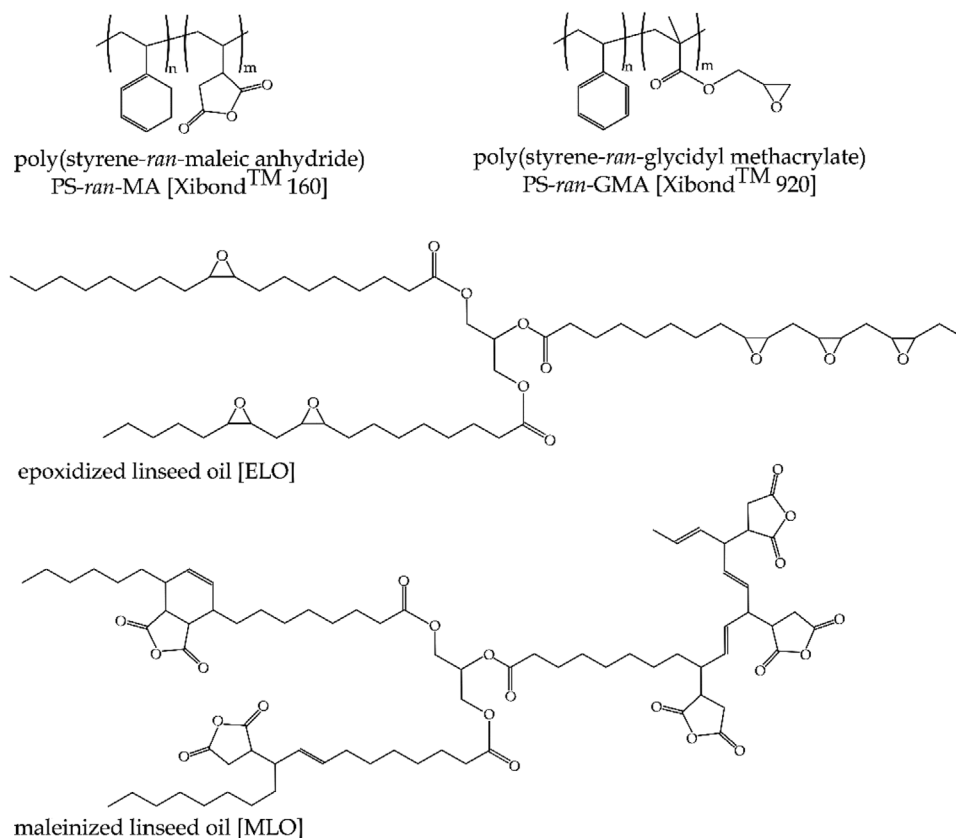
Characterization of PLA/PC Blends

Mechanical Characterization: Mechanical properties of PLA/PC blends were obtained using a universal testing machine ELIB 50 from S.A.E. Ibertest (Madrid, Spain) according to ISO 527-1:2012. A 5-kN load cell was used and the cross-head speed was set to 10 mm min^{-1}. Shore hardness was measured in a 676-D durometer from J. Bot Instruments (Barcelona, Spain), using the D-scale, on injection-molded samples with dimensions 80 × 10 × 4 mm^3, according to ISO 868:2003. Toughness was assessed by the impact Charpy test on injection-molded rectangular samples notched with dimensions 80 × 10 × 4 mm^3 in a 6-J pendulum from Metrotec S.A. (San Sebastián, Spain), following the guidelines of ISO 179–1:2010. All tests were performed at room temperature, that is, 25 °C, and at least six samples of each material were tested, and the characteristic parameters from each test were obtained and averaged.

Morphology of PLA/PC Blends: The morphology of the fracture surfaces from impact tests of the PLA/PC blends with different compatibilizers, was observed by FESEM in a ZEISS ULTRA 55 microscope from Oxford Instruments (Abingdon, UK), working at an acceleration voltage of 2 kV. Before placing the samples in the vacuum chamber, they were subjected to a sputtering process with a gold–palladium alloy in an EMITECH sputter coating SC7620 from Quorum Technologies, Ltd. (East Sussex, UK).

Thermal Characterization of PLA/PC Blends: The main thermal transitions of PLA/PC blends were obtained by DSC in a Mettler-Toledo 821 calorimeter (Schwerzenbach, Switzerland). To obtain reliable measurements, the sample size ranged from 5 to 7 mg. All samples were subjected to a three-step temperature program consisting on a first heating step from 20 °C to 180 °C, followed by cooling to 0 °C. After this, a second heating ramp from 0 °C to 350 °C was programmed. The heating and cooling rates were 10 °C min^{-1} for all three thermal steps. All DSC tests were run in triplicate using nitrogen atmosphere with a flow rate of 66 mL min^{-1} using standard sealed aluminium crucibles with a capacity of 40 μL.

TGA was performed in a LINSEIS TGA 1000 (Selb, Germany). The sample weight for TGA analysis ranged from 5 to 7.5 mg. Samples were placed in standard alumina crucibles with a capacity of 70 μL and subjected to a

**ADVANCED
SCIENCE NEWS**

www.advancedsciencenews.com

Macro-
molecular
Materials and Engineering
www.mame-journal.de

poly(styrene-*ran*-maleic anhydride)
PS-*ran*-MA [Xibond™ 160]

poly(styrene-*ran*-glycidyl methacrylate)
PS-*ran*-GMA [Xibond™ 920]

epoxidized linseed oil [ELO]

maleinized linseed oil [MLO]

Scheme 1. Chemical structure of different compatibilizers for polylactide (PLA)/polycarbonate PC blends with maleic anhydride and glycidyl functionalities.

Table 5. Summary of compositions according to the weight content (wt%) of polylactide (PLA)/polycarbonate (PC) and different compatibilizers and additives.

Code	PLA [wt%]	PC [wt%]	Xibond 920 [phr[a]]	Xibond 160 [phr]	ELO [phr]	MLO [phr]
PLA	100	0	0	0	0	0
PC	0	100	0	0	0	0
PLA/PC	80	20	0	0	0	0
PLA/PC/Xibond920	80	20	2.5	0	0	0
PLA/PC/Xibond160	80	20	0	2.5	0	0
PLA/PC/ELO	80	20	0	0	5	0
PLA/PC/MLO	80	20	0	0	0	5

[a] phr stands for the weight parts of the additive per one hundred weight parts of the base PLA/PC blend.

heating ramp from 30 °C to 700 °C at a heating rate of 10 °C min^{-1} in air atmosphere. In addition to the mass loss curves, the first DTG curves were also collected, showing the weight loss rate as a function of the increasing temperature. All TGA tests were carried out in triplicate.

Dynamic-Mechanical Thermal Analysis (DMTA) of PLA/PC Blends: DMTA of PLA/PC blends was carried out in a DMA1 dynamic analyzer from Mettler-Toledo (Schwerzenbach, Switzerland), working in single cantilever flexural conditions. Rectangular samples with dimensions 20 × 6 × 2.7 mm^3 were subjected to a dynamic temperature sweep from 30 °C to 140 °C at a constant heating rate of 2 °C min^{-1}. The selected frequency was 1 Hz and the maximum cantilever deflection for the dynamic test was set to 10 μm. All DMTA tests were made in triplicate.

Color and Contact Angle Measurements: A Konica CM-3600d Colorflex-DIFF2 colorimeter, from Hunter Associates Laboratory, Inc. (Reston, VA,

USA) was used for the color measurement. Color coordinates CIELab (L*, a*, and b*) were measured according to the following criteria: L* represents the lightness and ranges from 0 to 100; a* stands for the green (a* < 0) to red (a* > 0) color coordinate, while b*, represents the blue (b* < 0) to yellow (b* > 0) color coordinate. The yellowing index of each sample was calculated according to the ASTM E313. Color measurements were carried out on standard dog-bone samples. Measurements were repeated at least 10 times and the color coordinates were averaged.

Contact angle measurements were carried out with an EasyDrop Standard goniometer model FM140 from KRÜSS GmbH (Hamburg, Deutschland) which is equipped with a video capture kit and analysis software Drop Shape Analysis SW21; DSA1). Double distilled water was used as test liquid. Wettability properties were studied on the surface of rectangular samples with dimensions 80 × 10 × 4 mm^3. At least, 10

measurements were obtained, and the corresponding water contact angles were averaged.

Conflict of Interest

The authors declare no conflict of interest.

Data Availability Statement

Data available on request from the authors.

[1] N. Kawashima, T. Yagi, K. J. M. M. Kojima, *Engineering* **2019**, *304*, 1900383.

[2] R. J. H. Scalenghe, *Heliyon* **2018**, *4*, e00941.

[3] N. Yarahmadi, I. Jakubowicz, J. Enebro, *J. Appl. Polym. Sci.* **2016**, *133*, 43916.

[4] M. Nofar, D. Sacligil, P. J. Carreau, M. R. Kamal, M.-C. Heuzey, *Int. J. Biol. Macromol.* **2019**, *125*, 307.

[5] T. Mukherjee, N. Kao, *J. Polym. Environ.* **2011**, *19*, 714.

[6] O. Martin, L. Avérous, *Polymer* **2001**, *42*, 6209.

[7] J. S. Lee, G. H. Hwang, Y. S. Kwon, Y. G. Jeong, *Engineering* **2021**, 2100122.

[8] Y. Geng, H. He, H. Liu, H. Jing, *Polym. Adv. Technol.* **2020**, *31*, 2848.

[9] A. A. Yussuf, I. Massoumi, A. Hassan, *J. Polym. Environ.* **2010**, *18*, 422.

[10] B. L. Shah, S. E. Selke, M. B. Walters, P. A. Heiden, *Polym. Compos.* **2008**, *29*, 655.

[11] K.-W. Kim, B.-H. Lee, H.-J. Kim, K. Sriroth, J. R. Dorgan, *J. Therm. Anal. Calorim.* **2012**, *108*, 1131.

[12] S. Pilla, S. Gong, E. O'Neill, R. M. Rowell, A. M. J. P. E. Krzysik, *Science* **2008**, *48*, 578.

[13] A. P. Mathew, K. Oksman, M. Sain, *J. Appl. Polym. Sci.* **2005**, *97*, 2014.

[14] J. R. Dios, B. Gonzalo, C. R. Tubio, J. Cardoso, S. Gonçalves, D. Miranda, V. Correia, J. C. Viana, P. Costa, S. Lanceros-Méndez, *Macromol. Mater. Eng.* **2020**, *305*, 2000379.

[15] J. B. Lee, Y. K. Lee, G. D. Choi, S. W. Na, T. S. Park, W. N. J. P. D. Kim, *Stability* **2011**, *96*, 553.

[16] Y. Wang, S. M. Chiao, T. F. Hung, S. Y. Yang, *J. Appl. Polym. Sci.* **2012**, *125*, E402.

[17] P. Jariyasakoolroj, K. Tashiro, W. Chinsirikul, N. Kerddonfag, S. J. M. M. Chirachanchai, *Engineering* **2019**, *304*, 1900340.

[18] B. Imre, K. Renner, B. Pukanszky, *eXPRESS Polym. Lett.* **2014**, *8*, 2.

[19] I. N. H. M. Haneef, Y. F. Buys, N. M. Shaffiar, N. A. Haris, A. M. A. Hamid, S. I. S. J. P. E. Shaharuddin, *Science* **2020**, *60*, 2876.

[20] E. Ruiz-Silva, M. Rodríguez-Ortega, L. C. Rosales-Rivera, F. J. Moscoso-Sánchez, D. Rodrigue, R. González-Núñez, *Polymers* **2021**, *13*, 217.

[21] I. Keridou, J. Cailloux, J. C. Martínez, O. Santana, M. L. Maspoch, J. Puiggalí, L. Franco, *Polymer* **2020**, *202*, 122676.

[22] Z. Bai, Q. Dou, *J. Polym. Environ.* **2018**, *26*, 959.

[23] Y. Xu, J. Loi, P. Delgado, V. Topolkaraev, R. J. McEneany, C. W. Macosko, M. A. Hillmyer, *Ind. Eng. Chem. Res.* **2015**, *54*, 6108.

[24] P. Choudhary, S. Mohanty, S. K. Nayak, L. Unnikrishnan, *J. Appl. Polym. Sci.* **2011**, *121*, 3223.

[25] M. Kaseem, Y. G. Ko, *J. Polym. Environ.* **2017**, *25*, 994.

[26] K. Hamad, M. Kaseem, F. Deri, Y. G. Ko, *Mater. Lett.* **2016**, *164*, 409.

[27] S. Hazer, M. Coban, A. Aytac, *J. Appl. Polym. Sci.* **2018**, *135*, 46881.

[28] F. Hedayati, N. Moshiri-Gomchi, M. Assaran-Ghomi, S. Sabahi, N. Bahri-Laleh, S. Mehdipour-Ataei, J. Mokhtari-Aliabad, S. A. Mirmohammadi, *Polym. Adv. Technol.* **2020**, *31*, 566.

[29] L. Lin, C. Deng, G.-P. Lin, Y.. Wang, *Ind. Eng. Chem. Res.* **2015**, *54*, 5643.

[30] L. Lin, C. Deng, Y.-Z. Wang, *Polym. Adv. Technol.* **2015**, *26*, 1247.

[31] C. Liu, S. Lin, C. Zhou, W. Yu, *Polymer* **2013**, *54*, 310.

[32] V. T. Phuong, M.-B. Coltelli, P. Cinelli, M. Cifelli, S. Verstichel, A. Lazzeri, *Polymer* **2014**, *55*, 4498.

[33] L. Quiles-Carrillo, N. Montanes, C. Sammon, R. Balart, S. Torres-Giner, *Ind. Crops Prod.* **2018**, *111*, 878.

[34] F. Yemisci, A. Aytac, *Fibers Polym.* **2017**, *18*, 1445.

[35] N. Chelghoum, M. Guessoum, M. Fois, N. Haddaoui, *J. Polym. Environ.* **2018**, *26*, 342.

[36] Z. Qu, J. Bu, X. Pan, X. Hu, *J. Polym. Res.* **2018**, *25*, 138.

[37] F. Hassouna, J.-M. Raquez, F. Addiego, P. Dubois, V. Toniazzo, D. Ruch, *Eur. Polym. J.* **2011**, *47*, 2134.

[38] T. Kanzawa, K. Tokumitsu, *J. Appl. Polym. Sci.* **2011**, *121*, 2908.

[39] Y. Zhou, L. Luo, W. Liu, G. Zeng, Y. J. A. I. M. S. Chen, *Engineering* **2015**, *6*, 393582.

[40] V. Nagarajan, A. K. Mohanty, M. Misra, *ACS Sustainable Chem. Eng.* **2016**, *4*, 2899.

[41] B. Chieng, N. Ibrahim, Y. Then, Y. Loo, *Molecules* **2014**, *19*, 16024.

[42] J. F. Balart, V. Fombuena, O. Fenollar, T. Boronat, L. Sánchez-Nacher, *Composites, Part B* **2016**, *86*, 168.

[43] A. Carbonell-Verdu, D. Garcia-Garcia, F. Dominici, L. Torre, L. Sanchez-Nacher, R. Balart, *Eur. Polym. J.* **2017**, *91*, 248.

[44] J. M. Ferri, D. Garcia-Garcia, L. Sánchez-Nacher, O. Fenollar, R. Balart, *Carbohydr. Polym.* **2016**, *147*, 60.

[45] J. M. Ferri, D. Garcia-Garcia, N. Montanes, O. Fenollar, R. Balart, *Polym. Int.* **2017**, *66*, 882.

[46] B. N. Jang, C. A. Wilkie, *Thermochim. Acta* **2005**, *426*, 73.

[47] L. Song, Q. He, Y. Hu, H. Chen, L. Liu, *Polym. Degrad. Stability* **2008**, *93*, 627.

[48] M. Cristea, D. Ionita, M. M. Iftime, *Materials* **2020**, *13*, 5302.

[49] V. T. Phuong, M. B. Coltelli, I. Anguillesi, P. Cinelli, A. Lazzeri, in *AIP Conf. Proc.*, American Institute of Physics, **2014**, p. 142.

[50] J. F. Balart, N. Montanes, V. Fombuena, T. Boronat, L. Sánchez-Nacher, *J. Polym. Environ.* **2018**, *26*, 701.

[51] E. A. Vogler, *Adv. Colloid Interface Sci.* **1998**, *74*, 69.